Accurate People Counting Based on Radar: Deep Learning Approach

Jae-Ho Choi, Ji-Eun Kim, Nam-Hoon Jeong, and Kyung-Tae Kim
Dept. Electrical Engineering,
Pohang University of Science and Technology
Pohang, Gyeongbuk, KOREA
jhchoi93@postech.ac.kr, jieun7@postech.ac.kr,
sonata@postech.ac.kr, kkt@postech.ac.kr

Seung-Hyun Jin
Land Systems Research Team 1
Defence Agency for Technology and Quality
Jinju, Gyeongnam, KOREA
jinsh@dtaq.re.kr

***Abstract*—In this study, a novel radar-based people counting (PC) method is presented using the deep learning (DL) approach. The DL algorithm is a great tool that enables the automatic formation of the optimal features; however, it must be utilized carefully, considering the domain knowledge to prevent the concerns of learning unnecessary information, followed by overfitting. To address the problem and successfully apply the DL framework to the radar-based PC, we propose three novel solutions. First, we establish the preprocessing pipelines to transform the raw signals into a suitable form for network inputs. Second, a network architecture is newly proposed considering the radar signal characteristics and PC application. Finally, we propose several data augmentation strategies to artificially increase the size of training data. It was observed from experiments using real measured data that the proposed DL-based PC approach outperforms the conventional PC methods.**

Keywords—People counting, deep learning, preprocessing, recurrent neural network, data augmentation

I. Introduction

People counting (PC) is a promising technique to obtain the density information of the crowd in a certain area. Due to the ability of PC to automatically detect the number of people even when they move around freely, it can be used in various internet of things (IoT) technologies such as security systems and resource management systems in the future smart buildings [1] [2]. In particular, using radar as a sensor, it is achievable to design a PC system that is robust in light changes and free from privacy invasion, which are great benefits over cameras. Consequently, there is an increasing demand for the use of radars in PC applications [3]–[7].

The radar-based PC algorithms have generally been implemented using the feature-based machine learning (FML) framework. Specifically, meaningful features are developed from a set of received radar signals, and then a linear or nonlinear classifier is trained based on the features and corresponding labels (i.e., the number of people). Finally, the trained classifier is able to estimate the number of people from newly reflected signals. To achieve reliable performance for the FML-based framework, it is essential to design elaborate features to ensure that each reflected signal is well-separated according to its label on the projected feature space. However, it is extremely challenging to manually design such robust features considering the various complexities that occur in PC, such as low signal-to-noise ratio (SNR) of human signals, overlapping among people, and irregular multipath signals.

Recently, the deep learning (DL) framework has been widely investigated for radar fields owing to its potential for the automatic extraction of optimal features, leading to considerable performance improvements in various applications such as the classification of radar images or micro-Doppler signatures [8]–[10]. In PC, Yang *et al*. [5] suggested employing the convolutional neural network (CNN) framework as is in image classification by regarding sequential raw signals as an image. However, this method failed to outperform the FML-based PC techniques because domain knowledge was not fully considered in the algorithm. Furthermore, appropriate preprocessing techniques were not applied, making it highly vulnerable to clutter changes. Motivated by this, we present a novel method to successfully apply the DL framework on the radar-based PC by resolving the aforementioned issues. First, we establish the preprocessing pipelines of raw received signals to form optimal inputs for a network. Next, we design a new network architecture, called PCNet, considering the inherent property of radar data, which is based on the bidirectional recurrent neural network (Bi-RNN) instead of the CNN. Finally, to relive the data deficiency problem while training the large-sized network, we develop data augmentation strategies based on the domain knowledge of our objective. Several experiments using an impulse radio ultra-wideband (IR-UWB) radar, a low-power radar suitable for indoor applications, were carried out in two different indoor environments when up to ten people were moving around freely. The proposed DL-based method was able to estimate the number of people with 91.6% in an open space and 76.1% in a closed space, which highly outperforms the conventional PC methods [5]–[7].

This paper is organized as follows: the proposed PC method including the implementation of preprocessing pipelines and the DL-based approach are discussed in detail in Section II. The experimental results of the measured data using an IR-UWB radar are presented in Section III. Finally, the conclusion is described in Section IV.

II. Proposed People Counting Framework

A. IR-UWB Radar Signal

An IR-UWB radar transmits an impulse-like signal and receives the reflected components from surroundings, where the received signal can be represented as a linear combination of the delayed signals as follows:

This research was supported by Energy Cloud R&D Program through the National Research Foundation of Korea (NRF) funded by the Ministry of Science, ICT (NRF-2019M3F2A1073402).

978-1-7281-8942-0/20/$31.00 ©2020 IEEE

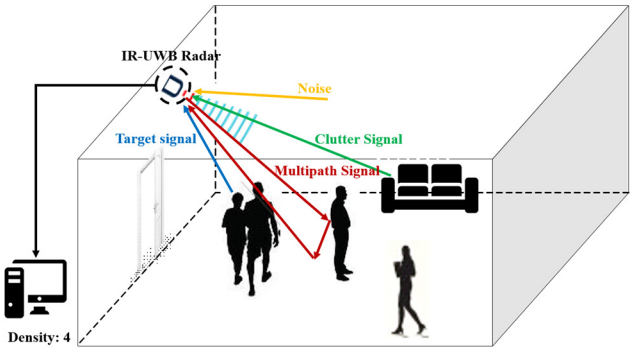

Fig. 1. Conceptual layout of people counting system using IR-UWB radar.

$$r_k(t) = \sum_p \sigma_p s(t-\tau_p) + n(t). \quad (1)$$

Here, $r_k(t)$ is the received signal at the slow time k, and $s(t)$ is the transmitted signal of the IR-UWB radar. σ_p and τ_p denote the amplitude and delay factors, respectively, which are determined by the radar cross section (RCS) and radar line of sight (RLOS) range of each scatterer p, respectively. $n(t)$ represents the noise component.

It should be noted that the received signals of the IR-UWB radar include not only human signals but also undesirable components, such as clutter, multipath, and noise, which disturb accurate PC (Fig. 1). These components induce numerous false alarms, resulting in significant difficulties in terms of the classifier. In other words, a large amount of training data will be required for a DL network to compose credible features taking into account all such false alarm errors.

B. Preprocessing Pipelines

In order to mitigate the concern of data requirements and stabilize the network performance, appropriate preprocessing must be applied to the reflected signals before training. Therefore, we developed preprocessing pipelines for the IR-UWB radar signals based on the domain knowledge of the algorithm. Following the aforementioned discussions, the objective of the preprocessing stage is to suppress the unwanted components and uncertainties from the raw received signals as much as possible and form optimal inputs in terms of the DL network. Specifically, the preprocessing pipelines consist of DC removal, clutter elimination (CE), matched filtering (MF), resizing, and standardization.

Let the discretized signal of k-th received signal $r_k(t)$ be

$$\mathbf{r}_k = [r_k(t_1), r_k(t_2), \ldots, r_k(t_i), \ldots, r_k(t_{N_r})]^T, \quad (2)$$

where $[t_1, t_2, \ldots, t_{N_r}]$ is the sampling time instant and N_r is the total number of samples in the fast time domain. The DC offset is removed from each discretized signal so that each DC offset of the received pulse remains consistent:

$$\mathbf{r}_k^{DC} = \mathbf{r}_k - \frac{1}{N_r}\sum_{i=1}^{N_r} r_k(t_i). \quad (3)$$

Next, we eliminate the clutter components in the DC-removed signal $\mathbf{r}_k^{DC}$ using a reference method (RM). The RM method subtracts the reference signal, collected in advance, from each received pulse as follows:

$$\mathbf{r}_k^{CE} = \mathbf{r}_k^{DC} - \left(\mathbf{r}_{ref} - \frac{1}{N_r}\sum_{k=1}^{N_r} r_{ref}(t_k)\right), \quad (4)$$

where $\mathbf{r}_k^{CE}$ denotes the signal with its clutter components suppressed, and $\mathbf{r}_{ref}$ is the reference signal collected from an empty space without individuals. In [5], the authors concluded that the CE process rather degrades the PC performance by suppressing not only clutter components but also human components. However, from a number of experiments, we found the great advantage of RM, where there is no risk of suppressing human components together [11], and found its great usefulness.

After CE, MF is performed to deal with noise components. By convolving with the transmitted signal $\mathbf{s}$, the low SNR characteristics of the IR-UWB radar signals can be complemented as follows:

$$\mathbf{r}_k^{MF} = \mathbf{r}_k^{CE} * \mathbf{s}. \quad (5)$$

Next, each filtered signal $\mathbf{r}_k^{MF}$ is resized, preventing the network size from being too large and increasing computational efficiency. Let $f(\cdot)$ is the one-dimensional (1D) spline interpolation function [12] that resizes a certain N_r-length signal to $\tilde{N}_r$-length signal, then the output can be represented as follows:

$$\mathbf{r}_k^{RE} = f(\mathbf{r}_k^{MF}), \quad (6)$$

where $\mathbf{r}_k^{RE}$ is the k-th resized signal of length $\tilde{N}_r$ ($\tilde{N}_r \le N_r$). Following the resizing process, the consecutive preprocessed pulses are fused to form a frame so that the network estimates the number of people using a frame-by-frame basis instead of a pulse-by-pulse basis. Using several pulses to obtain a result, signal variation over time can also be considered. The k-th frame $\mathbf{F}_k \in \mathbb{R}^{\tilde{N}_r \times N_p}$ is formed using N_p preprocessed pulses as follows:

$$\mathbf{F}_k = \left[\mathbf{r}_k^{RE}\ \mathbf{r}_{k+1}^{RE} \cdots \mathbf{r}_{k+N_p-1}^{RE}\right]. \quad (7)$$

Finally, each element of the frame is standardized to have zero mean and unit variance as follows:

$$\left(\bar{\mathbf{F}}_k\right)_{i,j} = \frac{\left(\mathbf{F}_k\right)_{i,j} - \mathbb{E}[\mathbf{F}_k]}{\sqrt{\mathrm{Var}[\mathbf{F}_k]}} \quad (1 \le i \le \tilde{N}_r, 1 \le j \le N_p), \quad (8)$$

where $(\cdot)_{i,j}$ refers to the element in the i-th row and j-th column of the frame matrix, and $\bar{\mathbf{F}}_k$ is the k-th standardized frame. E[·] and Var[·] are estimated sample mean variance values, respectively.

C. PCNet Architecture

CNN is a reliable architecture suitable for finding meaningful representations of image data [13]. In the case of the preprocessed frame, each preprocessed pulse $\bar{\mathbf{r}}_k^{RE}$ within $\bar{\mathbf{F}}_k$ retains information about the number of people.

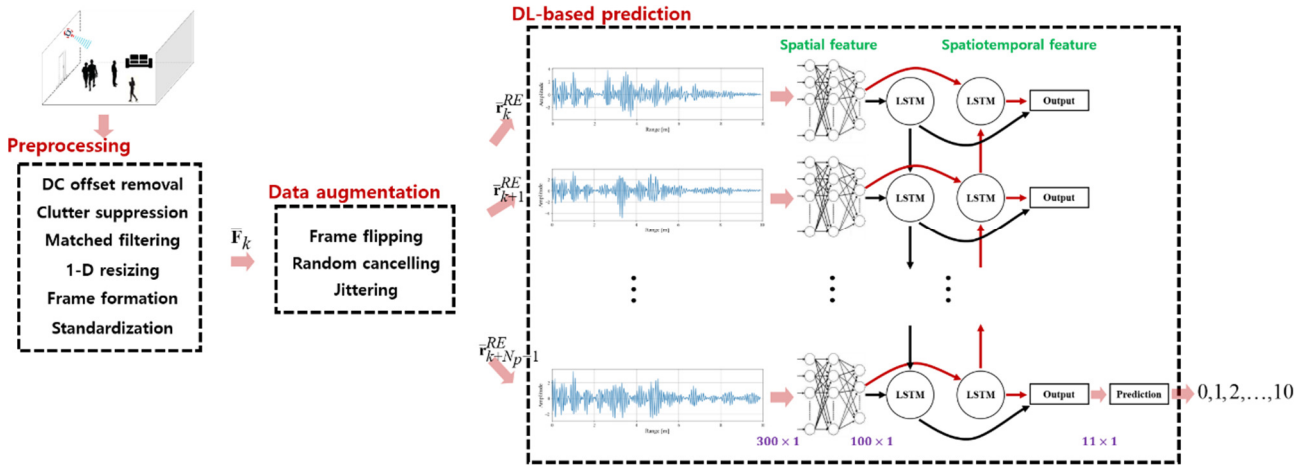

Fig. 2. Overall architecture of the proposed PC model.

Simultaneously, the number of people can also be inferred from the sequential changes of signals in a frame. Therefore, $\overline{\mathbf{F}}_k$ is more like a sequential series of 1D signals rather than a 2D image even if it has a 2D matrix form. Motivated by this, we developed a new network architecture based on BiRNN instead of CNN to better address the spatiotemporal characteristics of input frame data.

Fig. 2 shows the overall architecture of the proposed PCNet that estimates the number of people from each preprocessed frame. Let the k-th frame $\overline{\mathbf{F}}_k$ is an input of the network. First, the network independently extracts range-domain feature from each preprocessed signal in $\overline{\mathbf{F}}_k$ using a three-layer fully-connected (FC) network [13] with the number of nodes as 300, 300, and 100, respectively. From an arbitrary l-layer input $\mathbf{x}^{(l)} \in \mathbb{R}^{L\times 1}$, the output of the FC layer $\mathbf{x}^{(l+1)} \in \mathbb{R}^{\tilde{L}\times 1}$ is encoded as follows:

$$\mathbf{x}^{(l+1)} = \varphi\left(\mathbf{W}^{(l+1)}\mathbf{x}^{(l)} + \mathbf{b}^{(l+1)}\right), \tag{9}$$

where $\varphi(\cdot)$ is the exponential linear unit (ELU) activation function [14], and $\mathbf{W}^{(l+1)}$ and $\mathbf{b}^{(l+1)}$ are the weights and biases of the corresponding layer, respectively. The N_p preprocessed pulses in the frame are independently introduced to FC networks, followed by the nonlinear operation of several FC layers, and then N_p spatial features can be formed.

To further improve the performance, our network employs the Bi-RNN framework, so that the hidden sequential patterns in the frame data are considered as well. The Bi-RNN framework connects the N_p independent features in sequential order in the forward or backward direction. Here, if the frame size N_p increases, the earlier information of the sequence would be forgotten. This problem, known as the vanishing gradient descent, can be solved by using a long short-term memory (LSTM) unit [15] in each Bi-RNN node. At certain time step s, an LSTM unit calculates its hidden state $\mathbf{h}_{(s)}$ from the input vector $\mathbf{x}_{(s)}$ (in our case, extracted spatial feature from FC network), and the information from previous state $\mathbf{h}_{(s-1)}$ using a combination of nonlinear operations of input gate $\mathbf{i}_{(s)}$, output gate $\mathbf{o}_{(s)}$, and forget gate $\mathbf{f}_{(s)}$ as follows:

$$\begin{aligned}
\mathbf{i}_{(s)} &= \sigma(\mathbf{W}_{ix}\mathbf{x}_{(s)} + \mathbf{W}_{ih}\mathbf{h}_{(s-1)} + \mathbf{b}_i), \\
\mathbf{o}_{(s)} &= \sigma(\mathbf{W}_{ox}\mathbf{x}_{(s)} + \mathbf{W}_{oh}\mathbf{h}_{(s-1)} + \mathbf{b}_o), \\
\mathbf{f}_{(s)} &= \sigma(\mathbf{W}_{fx}\mathbf{x}_{(s)} + \mathbf{W}_{fh}\mathbf{h}_{(s-1)} + \mathbf{b}_f), \\
\mathbf{g}_{(s)} &= \tanh(\mathbf{W}_{gx}\mathbf{x}_{(s)} + \mathbf{W}_{gh}\mathbf{h}_{(s-1)} + \mathbf{b}_g), \\
\mathbf{a}_{(s)} &= \mathbf{f}_{(s)} \cdot \mathbf{a}_{(s-1)} + \mathbf{i}_{(s)} \cdot \mathbf{g}_{(s)}, \\
\mathbf{h}_{(s)} &= \mathbf{o}_{(s)} \cdot \tanh(\mathbf{a}_{(s)}),
\end{aligned} \tag{10}$$

where $\sigma(\cdot)$ is the sigmoid function, and $\mathbf{W}$ and $\mathbf{b}$ are the weights and biases of corresponding gates, which need to be learned during the training phase. Then, the spatiotemporal features of the input frame $\overline{\mathbf{F}}_k$ are comprehensively integrated into the final state of the Bi-RNN. Finally, the number of people can be estimated by applying a softmax classifier [13] to the output state of the final time step.

D. Network Training

It should be noted that the DL-based framework requires large training datasets to generalize numerous internal parameters. However, it is substantially laborious to acquire sufficient datasets for radar-based PC applications because many people are needed to collect every received pulse, and the characteristics of the reflected signals vary greatly depending on their spatial distribution. To relieve the data deficiency problem, we augmented the training data considering our domain knowledge.

First, given each preprocessed frame, we flipped the frame in the slow time domain. This implies that the number of people in a frame remains unchanged even if the direction of each individual is reversed. Second, a certain part of each pulse was randomly removed (i.e., set to zero) from each preprocessed pulse in a frame. At this time, the length of the removed part was set to the average shoulder width of a person. This means that the number of people will remain the same even if the levels of human signals are very low for some pulses in a frame. Finally, we randomly added the Gaussian jitters to frames, making the network robust on noise components.

Based on the augmented frame data and corresponding target labels, a supervised learning scheme can be applied to train the network. Given a labeled training dataset of M samples, $\{(\overline{\mathbf{F}}_i, \mathbf{y}_i), i=1,\ldots,M\}$, where $\mathbf{y}_i$ is the one-hot encoded true label (i.e., the number of people). The cost

function is defined as the cross-entropy loss between the real and predicted number of people as follows:

$$L(\omega) = -\frac{1}{M}\sum_{i=1}^{M} \mathbf{y}_i \log(P(\bar{\mathbf{F}}_i;\omega)), \quad (11)$$

where $P(\cdot)$ is the estimated output from the PCNet, which is composed of the trainable parameters ω. Then, using the Adam optimizer [16], weights and biases within the network are optimized to reduce the cost per each iteration.

III. Experimental Results

A. Experimental Settings

To evaluate the effectiveness of the algorithm, several experiments were performed based on the real data in two different indoor environments. Fig. 3 shows the detail of each experimental environment. One experiment was performed in a lobby that is an open environment with a high ceiling and no walls (Fig. 3a). The other experiment was performed in a hall that is a relatively closed indoor environment with a low ceiling and side walls (Fig. 3b).

In each experiment, zero to ten people moved around freely within the beamwidth of the radar that is a fan-shaped space with a radius of 10 m and a central angle of 80°. A commercial IR-UWB radar (X4M03, Novelda, Norway), whose specifications are shown in Table I, was set up at about 2 m height at the apex of each space to collect reflected signals from the individuals. From each experimental space, we constructed training datasets by collecting the reflected pulses for 10 min per each number of people (0 to 10). After a week, we reinstalled the radar at almost the same location and re-collected the reflected signals for 5 min per each number of people for test datasets. For each measurement, subjects were chosen arbitrarily among a total of 16 participants. By doing so, we can evaluate the PC algorithm in consideration of the time and appearance variations, as well as minute changes in radar installation positions.

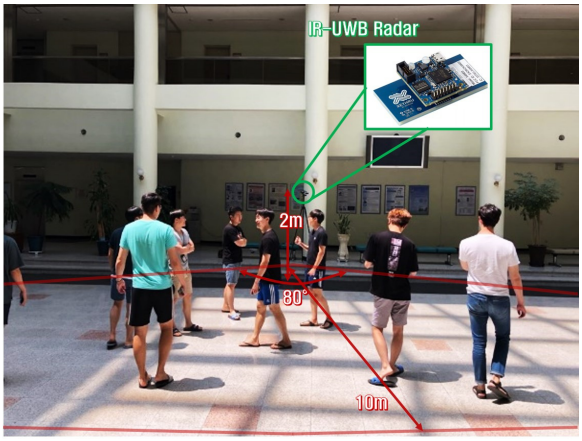

(a)

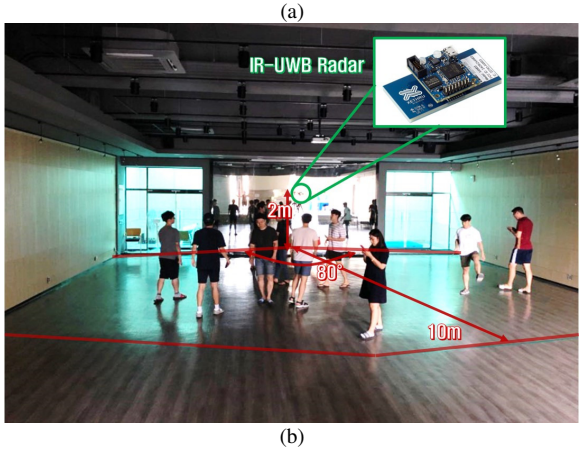

(b)

Fig. 3. Experimental environment: (a) open indoor space, (b) close indoor space

Using the constructed datasets, we applied the proposed preprocessing techniques with frame size N_p=25, and then trained our network based on an NVIDIA Titan RTX GPU. For hyper-parameters, a learning rate of 0.0001 and mini-batches of size 6 4 were used. In addition, the dropout technique [17] with the probability of 0.5 was applied to each FC layer to mitigate the overfitting problem.

B. Main Results

Table II summarizes the performance (i.e., test accuracy) comparisons between the conventional PC methods and the proposed PC model. Also, the results of applying only fractions of the proposed framework are shown to verify the efficacy of the developed preprocessing pipelines, network architecture, and data augmentation strategies.

Compared to the conventional PC methods [5]–[7], the proposed DL-based PC model predicts the number of people with much higher accuracies in both open and closed spaces. In particular, compared to the current state-of-the-art PC method [7], the proposed model shows 10.7% and 6.5% improvements in an open indoor space and a closed indoor space, respectively.

It is remarkable that the method in [5] presents substantially low accuracies. This is due to the fact that the CNN learns clutter-specific information that accounts for most of the raw reflected signals, making it highly vulnerable to even slight changes in clutter due to changes in the installed location of the radar. However, it can be observed that by applying proper preprocessing techniques, the CNN is able to extract features robust on slight clutter changes and

TABLE I
X4M03 IR-UWB Radar Specifications

Carrier frequency	7.29 GHz
Frequency bandwidth	1.5 GHz
Pulse repetition frequency	50 Hz
Power consumption	500mW >
Pulse width	65.8 ns
Interface	USB

TABLE II
Performance (Test Accuracy, %) Comparison of Conventional PC Methods and Proposed Model.

Type	People Counting Method	Accuracy in open space (%)	Accuracy in closed space (%)
DL	Raw + CNN [5]	20.8	9.7
FML	CLEAN + Maximum Likelihood [6]	69.9	58.7
FML	Hybrid feature + Random forest [7]	80.9	69.6
DL	Preprocessing + CNN	80.1	66.8
DL	Preprocessing + PCNet	85.7	72.1
DL	Preprocessing + PCNet + Data augmentation	**91.6**	**76.1**

successfully employ the potential of the DL algorithm, representing 59.3% and 57.1% improvements in the open and closed spaces, respectively. In addition, it should be noted that the capabilities of the network can be further improved by substituting the CNN architecture with the PCNet one and applying the proposed data augmentation techniques.

Tables III and IV represent the normalized confusion matrices of each test dataset in the open and closed indoor spaces, respectively. In each confusion matrix, the colors blue, yellow, and red denote the exact estimations, errors of a person, and errors of two or more people, respectively. The results indicate that the proposed PC algorithm perform better in an open space than in a closed space owing to more complex multipath characteristics in the closed environment. Nevertheless, the results also reveal that the proposed PC algorithm can accurately predict the number of people in most cases, and even if it is incorrect, the algorithm can count within one or two errors, regardless of the environments.

IV. Conclusion

In this study, we developed a novel accurate radar-based PC method using the DL framework. DL is a useful algorithm that allows one to find the optimal features automatically, but it is likely to extract highly domain-specific features and is prone to overfitting problems. Therefore, it is impossible to achieve reliable performance using the DL algorithm as it is. To address this problem, we established the preprocessing pipelines for radar signals to suppress the undesirable components in the signals. In addition, a network architecture named PCNet is defined considering the domain knowledge. Finally, three data augmentation strategies for radar-based PC are proposed to artificially increment the training data and prevent overfitting of the network. In the experiments based on real data, we confirmed that the proposed PC model is able to provide much more accurate predictions compared to the conventional FML-based techniques [5]–[7].

TABLE III
Normalized Confusion Matrix in Open Indoor Space.

Predicted label (Number of people) \ True label (Number of people)	0	1	2	3	4	5	6	7	8	9	10
0	100	0	0	0	0	0	0	0	0	0	0
1	0	100	3.3	0	0	0	0	0	0	0	0
2	0	0	95.0	5.8	0.3	0	0	0	0	0	0
3	0	0	1.7	89.2	7.0	0	0	0	0	0	0
4	0	0	0	4.2	89.4	2.5	0	0	0	0	0
5	0	0	0	0.8	3.3	85.5	7.0	0	0	0	0
6	0	0	0	0	0	12.0	92.2	9.4	0	0	0
7	0	0	0	0	0	0	0.8	87.2	3.3	0	0
8	0	0	0	0	0	0	0	1.7	94.7	3.3	5.4
9	0	0	0	0	0	0	0	1.7	2.0	84.7	5.4
10	0	0	0	0	0	0	0	0	0	12.0	89.2

TABLE IV
Normalized Confusion Matrix in Closed Indoor Space.

Predicted label (Number of people) \ True label (Number of people)	0	1	2	3	4	5	6	7	8	9	10
0	100	0	0	0	0	0	0	0	0	0	0
1	0	98.7	4.2	0	0	0	0	0	0	0	0
2	0	1.3	88.2	17.4	0	0	0	0	0	0	0
3	0	0	7.6	78.1	2.2	0	0	0	0	0	0
4	0	0	0	4.5	85.7	11.5	1.7	0	0	0	0
5	0	0	0	0	10.4	68.4	23.8	0	0	0	0
6	0	0	0	0	1.7	15.9	56.4	21.7	0	0	0
7	0	0	0	0	0	4.2	14.4	62.6	5.8	0	3.7
8	0	0	0	0	0	0	3.7	15.7	70.8	6.5	3.3
9	0	0	0	0	0	0	0	0	18.9	66.5	31.2
10	0	0	0	0	0	0	0	0	4.5	27.0	61.8

References

[1] P. K. D. Pramanik, B. K. Upadhyaya, S. Pal, and T. Pal, "Internet of things, smart sensors, and pervasive systems: Enabling connected and pervasive healthcare," in *Healthcare Data Analytics and Management*, Elsevier, 2019, pp. 1–58.

[2] G. Hancke, B. Silva, and G. Hancke, Jr., "The role of advanced sensing in smart cities," *Sensors*, vol. 13, no. 1, pp. 393–425, Dec. 2012.

[3] S. Bartoletti, A. Conti, and M. Z. Win, "Device-free counting via wideband signals," *IEEE J. Sel. Areas Commun.*, vol. 35, no. 5, pp. 1163–1174, May 2017.

[4] J. W. Choi, X. Quan, and S. H. Cho, "Bi-directional passing people counting system based on IR-UWB radar sensors," *IEEE Internet Things J.*, vol. 5, no. 2, pp. 512–522, Apr. 2018.

[5] X. Yang, W. Yin, and L. Zhang, "People counting based on CNN using IR-UWB radar," in *2017 IEEE/CIC International Conference on Communications in China (ICCC)*, Qingdao, China, 2017, pp. 1–5.

[6] J. W. Choi, D. H. Yim, and S. H. Cho, "People counting based on an IR-UWB radar sensor," *IEEE Sens. J.*, vol. 17, no. 17, pp. 5717–5727, Sep. 2017.

[7] X. Yang, W. Yin, L. Li, and L. Zhang, "Dense people counting using IR-UWB Radar with a hybrid feature extraction method," *IEEE Geosci. Remote Sens. Lett.*, vol. 16, no. 1, pp. 30–34, Jan. 2019.

[8] B. Xue and N. Tong, "DIOD: Fast and efficient weakly semi-supervised deep complex ISAR object detection," *IEEE Trans. Cybern.*, vol. 49, no. 11 pp. 1–13, Nov. 2019.

[9] O. Kechagias-Stamatis and N. Aouf, "Fusing deep learning and sparse coding for SAR ATR," *IEEE Trans. Aerosp. Electron. Syst.*, vol. 55, no. 2, pp. 785–797, Apr. 2019.

[10] B. Jokanovic and M. Amin, "Fall detection using deep learning in range-Doppler radars," *IEEE Trans. Aerosp. Electron. Syst.*, vol. 54, no. 1, pp. 180–189, Feb. 2018.

[11] J. E. Kim, J. H. Choi, and K. T. Kim, "Robust detection of presence of people using IR-UWB radar in an indoor environments," unpublished.

[12] S. McKinley and M. Levine, "Cubic spline interpolation," *College of the Redwoods*, vol. 45, no. 1, pp. 1049–1060, 1998.

[13] I. Goodfellow, Y. Bengio, and A. Courville, *Deep learning*, MIT press, 2016.

[14] H. K. Vydana and A. K. Vuppala, "Investigative study of various activation functions for speech recognition," in *2017 Twenty-third National Conference on Communications (NCC)*, Chennai, India, 2017, pp. 1–5.

[15] K. Greff, R. K. Srivastava, J. Koutnik, B. R. Steunebrink, and J. Schmidhuber, "LSTM: A search space odyssey," *IEEE Trans. Neural Networks Learn. Syst.*, vol. 28, no. 10, pp. 2222–2232, Oct. 2017.

[16] D. P. Kingma and J. Ba, "Adam: a method for stochastic optimization," pp. 1–15, Dec. 2014.

[17] N. Srivastava, G. Hinton, A. Krizhevsky, I. Sutskever, and R. Salakhutdinov, "Dropout: A simple way to prevent neural networks from overfitting," *J. Mach. Learn. Res.*, vol. 15, pp. 1929–1958, 2014.